ISSN 0020-1685, Inorganic Materials, 2015, Vol. 51, No. 8, pp. 747–753. © Pleiades Publishing, Ltd., 2015.
Original Russian Text © E.N. Abramova, A.M. Khort, A.G. Yakovenko, V.I. Shvets, 2015, published in Neorganicheskie Materialy, 2015, Vol. 51, No. 8, pp. 815–822.

Nanopore Formation during Electrolytic Etching of Silicon in Hydrofluoric Acid Solutions

E. N. Abramova, A. M. Khort, A. G. Yakovenko, and V. I. Shvets

Moscow State University, Moscow, 119899 Russia

e-mail: anavenko@yandex.ru

Received December 8, 2014

Abstract—A stepwise scheme has been proposed for gaining insight into the nanopore formation process in silicon during electrolytic etching in hydrofluoric acid solutions. We have studied the influence of the concentration and nature of dopants (phosphorus, arsenic, and antimony) in silicon, current density, electric field strength, and etching time on the axial and radial pore sizes and the pore distribution density. The dopants have been shown to play a predominant role in the nanopore formation process. The shape and spatial orientation of nanopores in Si substrates with the (100) and (111) crystallographic orientations have been interpreted in terms of specific features of the electrochemical etching of silicon in hydrofluoric acid solutions, related to the action of the etching ion $(HF_2)^-$. The observed discrepancy between the experimentally determined and calculated radial nanopore sizes has been accounted for by the low probability ($\simeq$6.25%) of simultaneous interaction of the fluorine atoms of an $(HF_2)^-$ ion with the corresponding silicon atoms located at vertices of a cube of the crystal lattice.

DOI: 10.1134/S0020168515080014

INTRODUCTION

Recent years have seen increased interest in nanomaterials and related nanostructures, motivated first of all by the unique properties inherent in such materials, which allows them to be used in devices for a variety of practical applications. One such material is nanoporous silicon (NS). Possessing a diversity of attractive characteristics, such as a large inner surface area, unusual electronic structure, large adsorption capacity, and biocompatibility, NS has already found application in the fabrication of current microsources, matrices for various sensors and detectors, and a great diversity of medical and biotechnological research directions [1–4]. However, practical application of NS requires nanomaterials possessing certain characteristics: surface structure, nanostructured layer thickness, and radial and axial pore sizes. In view of this, the study of the pore formation process in silicon, which underlies the formation of nanostructured layers, and the electronic structure of the silicon surface, is of paramount importance.

Extensive studies concerned with nanopore formation conditions and the structure of NS layers [5–8] have shown that these factors are influenced by a rather large number of process parameters. The main factors are as follows: the conductivity type of the unprocessed silicon; the degree of doping with donor and acceptor impurities; the nature of the dopant; the crystallographic orientation of the substrate; the quality of substrate surface processing; the chemical composition of the etchant; the etching current, time, and temperature; and the illuminance of the substrate. However, it has not yet been found out with certainty which of the above factors determines the NS formation process. Results presented in different reports and describing nanopore and nanolayer formation processes on the whole are often contradictory [7–9], which suggests either that the processes have a more complex character or that one has failed to take into account other factors and processes occurring in parallel with the chosen ones in the course of etching. In connection with this, the parameters of the forming layers and nanopores in the process of their preparation are rather difficult to accurately predict. Given the complexity of the general nanopore formation and development process in Si and the fact that this process is influenced by many factors, it is reasonable to address this issue in several steps, choosing factors that determine a given step among the diversity of factors that influence the entire pore formation process.

The purpose of this work was to study the mechanism of nanopore formation in Si under the action of the $(HF_2)^-$ ion, which predominantly etches silicon at HF concentrations above 1 M [10].

EXPERIMENTAL

We used *n*- and *p*-type (KEF, KES, KEM, and KDB) silicon wafers with resistivities in the range ρ_{Si} = 0.01–100 Ω cm, oriented along the (100) and (111) crystallographic planes. The wafers were etched with a hydrofluoric acid solution (45 wt % HF) in water in

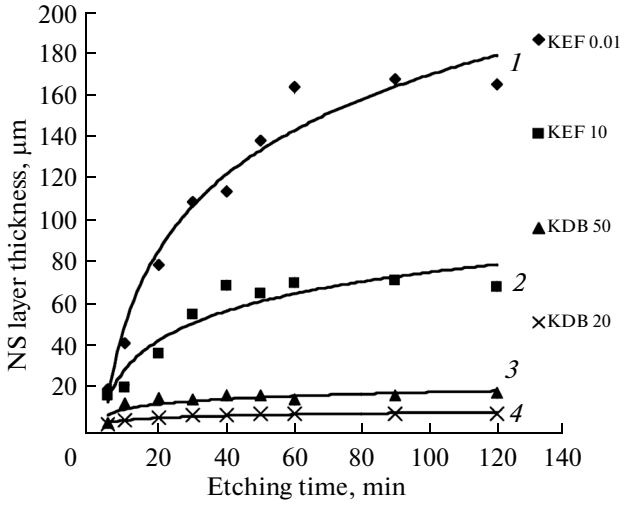

Fig. 1. Thickness of NS layers as a function of etching time at etching current densities of (*1*, *4*) 10 and (*2*, *3*) 30 mA/cm^2.

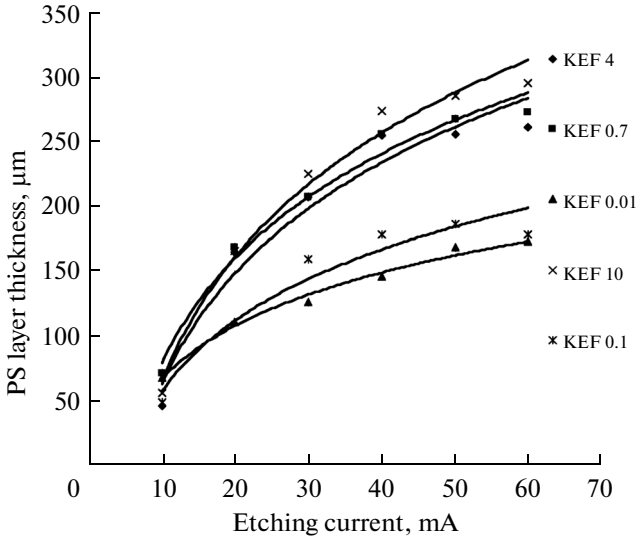

Fig. 2. Thickness of NS layers as a function of etching current: etching time, 60 min; (100)-oriented substrates.

the volume ratio 2 : 1 in a galvanostatic mode. The etching cell, made of Teflon, allowed for one-sided horizontal etching. The anode used was a polished massive copper plate, and the cathode had the form of a thin platinum plate. The electric field applied during etching was varied by using diaphragms of various sizes and changing the electrode separation.

The nanopore size, shape, and orientation and the thickness of NS layers were determined using a JEOL electron microscope and a POLAM R 312 optical microscope.

EXPERIMENTAL RESULTS

Our data on the effect of etching time on the thickness of nanostructured NS layers demonstrate (Fig. 1) that, for all samples, increasing the etching time leads to an increase in the thickness of the layer. In almost all instances, the largest increase in the thickness of the layers is observed during the first 20–25 min of etching. When the etching time increases further, to 120 min, the thickness of the layers increases substantially more slowly. A distinctive feature of the curves presented in Fig. 1 is that the thickness of the NS layers produced on the *n*-type silicon samples (curves *1*, *2*) considerably exceeds that on the *p*-type silicon samples (curves *3*, *4*). Increasing the etching current also increases the thickness of the NS layers (Fig. 2). This correlates well with previous results [11]. At optimal etching currents and durations, the maximum thickness of the NS layers produced on *p*-type silicon did not exceed 40–45 μm, whereas that on *n*-type silicon under identical conditions was 230–250 μm. The NS layers on the *p*-type substrates almost always cracked and peeled off from the surface immediately after drying, whereas this was not so on the *n*-type substrates (Fig. 3). These features are probably the consequence of the fact that different mechanisms underlie the silicon etching and nanopore formation processes in the *n*- and *p*-type samples. Given this, as well as the more pronounced formation of NS layers, which structurally have the form of individual pores in an *n*-type Si single crystal, and their high stability to environmental effects, the *n*-type samples were used in further studies.

Microscopic analysis showed that the structure of the NS layers produced on *n*-Si approached a system of individual nanopores in a single crystal (Fig. 4). The density of their distribution (Fig. 5) depended on electric field strength, which had a particularly strong effect on pore walls, whose thickness was comparable to or greater than the pore size.

Figure 6 plots the thickness of the NS layers against the resistivity of *n*-Si doped with various impurities (P, As, and Sb), and Fig. 7 presents such dependences for the thickness of the NS layers produced on KEF (phosphorus-doped) silicon at various etching times. In the resistivity range 0.01–5.0 Ω cm, the thickness of the layers increases monotonically, regardless of the nature of the sample and etching time. Note that the NS consists almost entirely of individual nanopores in the single crystal (Figs. 4, 5) and the pore size increases linearly (Fig. 8) with an increase in the resistivity of the substrate and a decrease in the density of the nanopore distribution.

Further increase in the resistivity of the silicon to $\rho > 5$–8 Ω cm is accompanied by an increase in the amorphous content of the surface region of the layers,

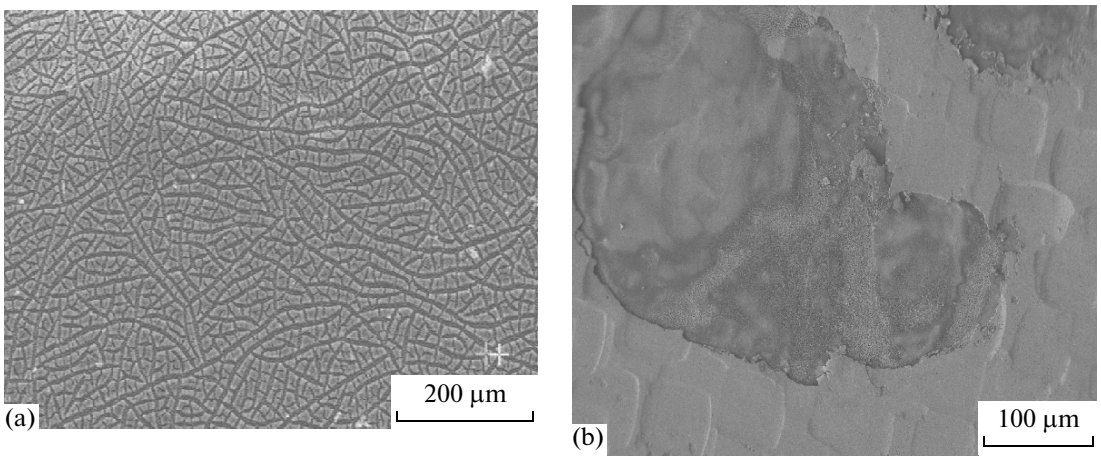

Fig. 3. Scanning electron microscope (SEM) images of the surface of NS layers on (a) *p*-type KDB 10 Si (1 h after preparation) and (b) *n*-type KEF 1 Si (100 h after preparation).

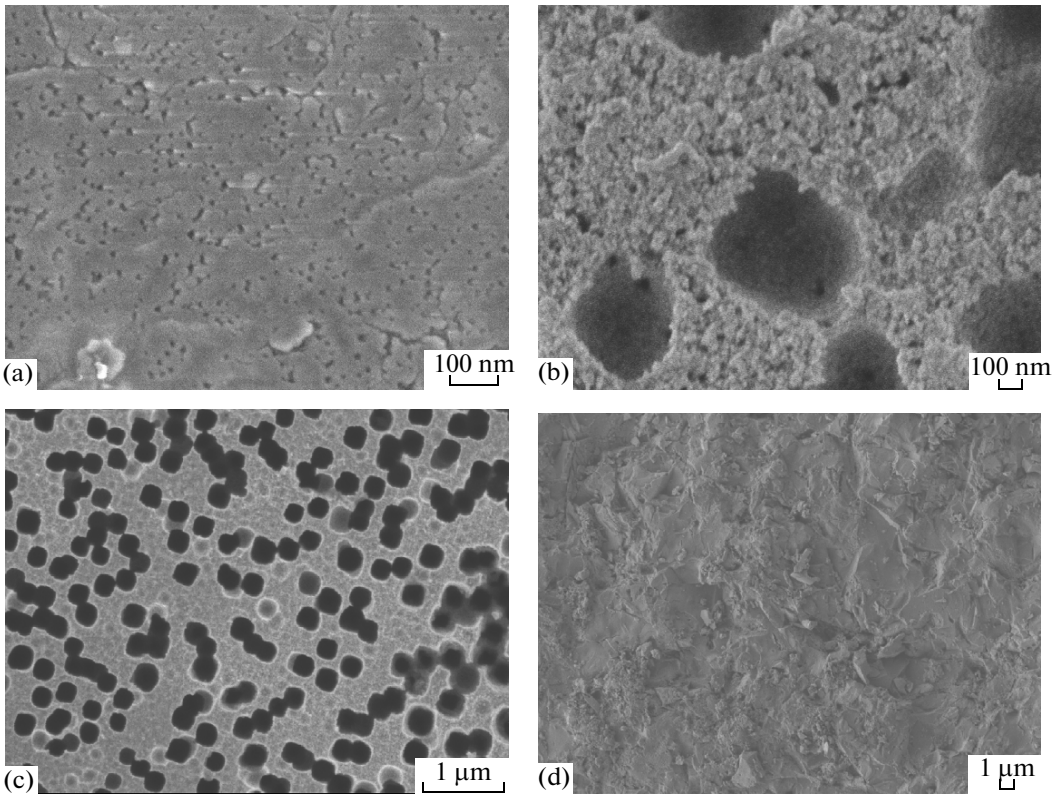

Fig. 4. SEM images of the surface of NS layers on (a) KEF 0.01, (b) KEF 5, (c) KEF 7.5, and (d) KEF 110.

whereas their thickness remains essentially unchanged (Figs. 4, 6, 7).

The present results demonstrate that the variation in the thickness of the NS layers, their structure, and the pore size are insensitive to the nature of the dopant in *n*-Si. At the same time, the doping impurity concentration at initial resistivities of silicon in the range 0.01–5 Ω cm has a significant effect on the thickness of the NS layers and the pore size (Figs. 1, 2, 7, 8). The etching current and time have no significant effect on the general character of the variation in the thickness of the layers (Figs. 1, 2, 7), whereas the electric field,

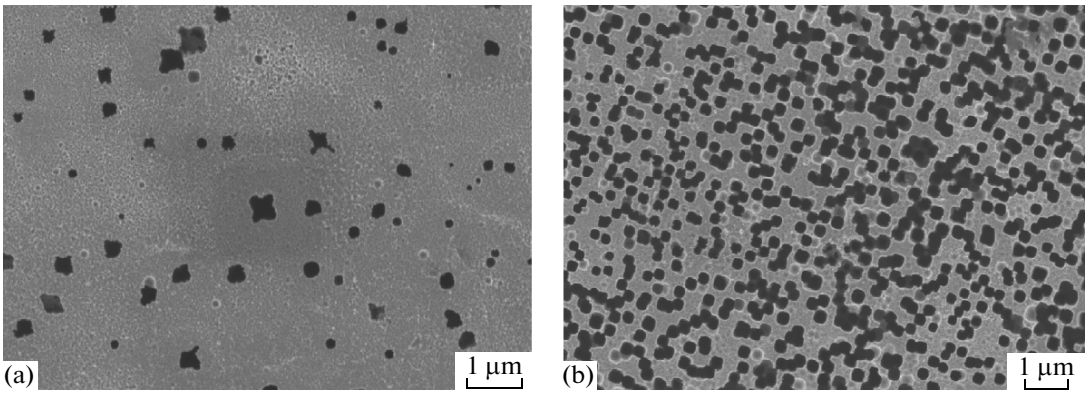

Fig. 5. SEM images of the surface of NS layers produced at different electric field strengths: (a) 10 and (b) 2.6 V/cm (KEF 7.5, (100) crystallographic orientation of the surface).

which ensures electrolytic etching, has a significant effect on the nanopore distribution density (Fig. 5).

DISCUSSION

The present results demonstrate that the degree of doping of silicon with P, As, and Sb donor impurities in the resistivity range 0.01–5.0 Ω cm has a crucial effect on the structuring of the NS layers and the pore distribution density.

These results can be interpreted as follows: Surface impurity atoms have a significant effect on the potential energy distribution of charge carriers in a two-dimensional chain of atoms on the silicon surface. With increasing impurity concentration (decreasing distance between impurity atoms), such distortions form a single system of a field with a periodically varying potential. Because of this, negatively charged etchant ions will tend to migrate to regions of a reduced negative surface potential of the substrate, producing pore nucleation sites there. With decreasing impurity concentration (increasing distance between impurity atoms), the structure of the electron potential energy distribution on the surface assumes a chaotic character, contributing to surface amorphization in the course of etching.

Using the NS layer thickness and the weight of the silicon removed by etching, we calculated the pore diameter as a function of the donor distribution density on the wafer surface (Fig. 8):

$$\Delta m_{Si} = [(\pi d_{pore}^2)/4]h_{layer}N_d\rho_{Si}, \quad (1)$$

where d_{pore} is the pore diameter, h_{layer} is the layer thickness, N_d is the donor distribution density on the wafer surface, ρ_{Si} is the density of single-crystal silicon, and Δm_{Si} is the weight of the silicon removed by etching.

According to Eq. (1), the pore diameter is proportional to $1/\sqrt{N_d}$, in agreement with previous results [11]. However, the experimentally determined nanop-

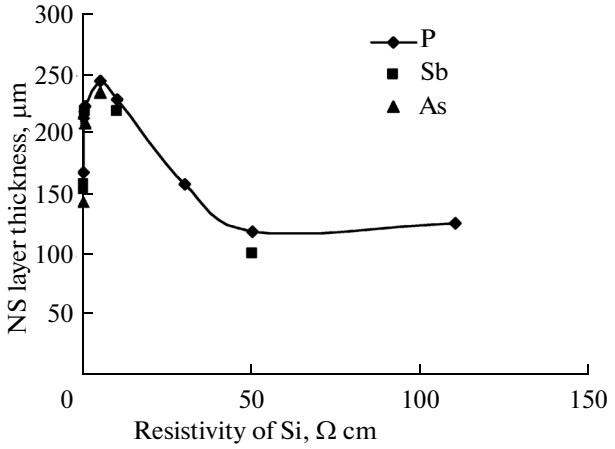

Fig. 6. Thickness of NS layers as a function of the resistivity of *n*-Si containing P, Sb, and As.

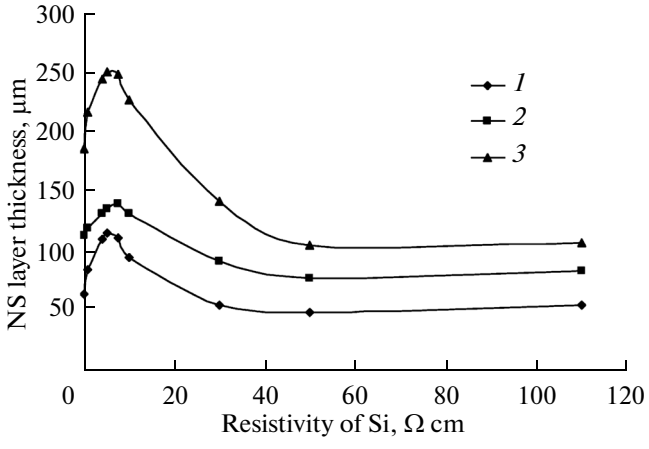

Fig. 7. Thickness of NS layers as a function of the resistivity of silicon (KEF) and etching time: etching current density of 50 mA/cm^2; etching time of (*1*) 15, (*2*) 30, and (*3*) 60 min.

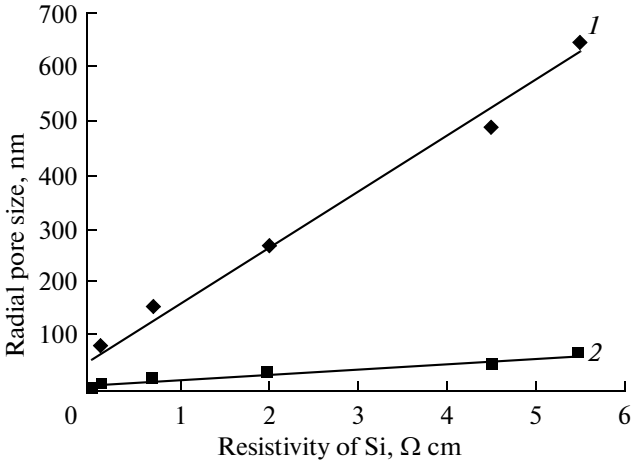

Fig. 8. Radial nanopore size as a function of the resistivity of the silicon at an etching current density of 25 mA and etching time of 30 min: (*1*) experimental data, (*2*) calculation results. The radial nanopore size was calculated for cylindrical nanopores. The difference between the values of the size of the area of the square and the corresponding rectangle close to the square does not exceed 12–15%.

ore size turned out to be a factor of 8–10 greater than the calculated one (Fig. 8). This may be related to specific features of the structure of the main etching ion $(HF_2)^-$ and the nature of the etching process for nanopore formation.

As shown earlier [10], pore formation in silicon is due to the presence of $(HF_2)^-$ ions in the etchant, whereas the presence of only F^- ions in the etchant (HF concentration < 1 M) does not cause pore formation. The $(HF_2)^-$ ion has an almost linear structure and is 2.27 Å in size [12, 13]. Given the above, the mechanism of the interaction between the $(HF_2)^-$ ion and silicon can be thought of as follows:

From the viewpoint of the relationship between its geometric size and the length of the Si–F bond (1.6 Å [13]) resulting from the interaction between one of the fluorine atoms of the $(HF_2)^-$ ion and a Si atom on a lattice site in silicon (with a lattice parameter of 5.43 Å [14]), the most likely interaction will be that of the two fluorine atoms of the $(HF_2)^-$ ion with Si atoms residing at vertices of a cube in the crystal lattice (1.6 Å + 2.27 Å + 1.6 Å ≃ 5.43 Å) (Fig. 9). Such interaction of the silicon atom 1 (Fig. 10a, atom Si1), partially ionized by one of the possible external influences (photon, heat, etc.), with one of the fluorine atoms of the $(HF_2)^-$ ion leads to the formation of a Si1–F covalent bond (Fig. 10b). According to Hund's rule, a new, unsaturated bond should form between the silicon atoms 2 and 3, and an electron not participating in chemical bonds between silicon atoms should form at atom Si2 (Fig. 10b). However, since atoms Si1 and Si5, which reside at vertices of a cube in the crystal lattice,

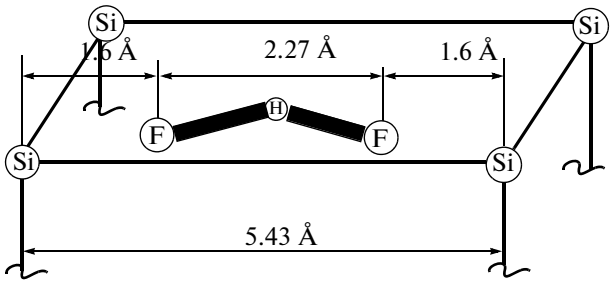

Fig. 9. Relationship between the unit-cell dimensions of Si, the size of the $(HF_2)^-$ ion, and the Si–F bond length.

are not linked by a direct chemical bond, to ensure interaction between the other fluorine atom of the $(HF_2)^-$ ion and atom Si5 (Fig. 10b), with allowance for geometric considerations (S–F bond length and $(HF_2)^-$ ion size (Fig. 9)), it is necessary that the new, unsaturated bond formed between atoms Si2 and Si3 pass to atom Si5 in the shortest way, through atoms Si3 and Si4 (Fig. 10b). Given that each Si atom has four bonds with other atoms, the probability of unsaturated bond switching in the direction indicated in Fig. 10 decreases from atom to atom.

We calculated the probability of the indicated transition of an unsaturated bond formed at atom Si1 to atom Si5. Since all possible transitions of the bond are equally probable, we have

$$A = 3P_1P_2P_3, \quad (2)$$

where A is the total probability of the event, P_1 is the probability that a new unsaturated bond will be located between two neighboring silicon atoms (Si2 and Si3), and P_2 and P_3 are the probabilities of its switching to a neighboring silicon atom (Si4 and Si5). The factor 3 reflects the equal probability of processes that, in accordance with the structure of the crystal lattice of silicon, may take three shortest paths from atom Si1 to atom Si5. Clearly, the probability P_2 is equal to P_3, so the formula for expressing event A takes the form

$$A = 3P_1P_2^2. \quad (3)$$

Using expression (3), we can calculate the probability of the switching of the unsaturated bond from atom Si1 to atom Si5. Since atom Si2 has one localized electron and one unsaturated bond, the bond may be located in one of three positions; the next two transitions of this bond are 1/4 because each next silicon atom has four bonds. Accordingly, the probability of event A is $A = 3 \times 1/3 \times (1/4)^2 = 0.0625$.

Thus, the probability of simultaneous interaction of two silicon atoms (Fig. 10, Si1, Si5) with the fluorine atoms of a $(HF_2)^-$ ion is 6.25%. It is worth pointing out that there is also a probability that an unsaturated bond between silicon atoms will switch to a

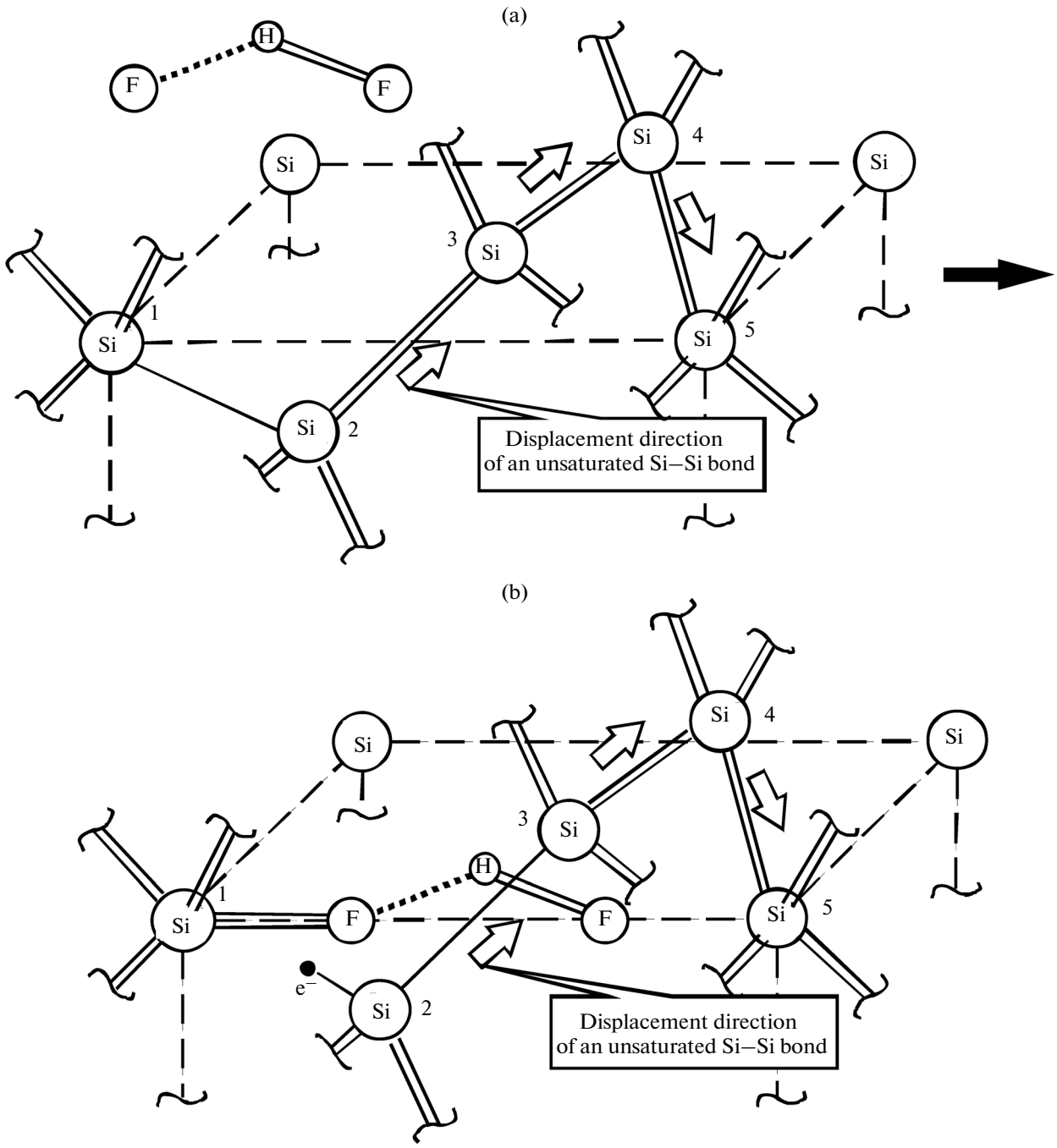

Fig. 10. Schematic diagram of possible interaction between the etching ion $(HF_2)^-$ and silicon atoms in the course of electrolytic etching.

neighboring Si atom at a cube vertex of the lattice not through the shortest path. This probability, however, will obviously be still lower in comparison with the calculated one. The fact that only 6.25% of the total number of $(HF_2)^-$ ions that reacted with Si simultaneously interact with silicon atoms by both of their fluorine atoms seems to account for the discrepancy between the calculated and experimentally determined radial nanopore sizes (Fig. 8).

Since, because of its linear structure, the $(HF_2)^-$ ion acts along the edges of the cubic lattice of silicon, the pore orientation in the bulk reflects the orientation of the silicon wafer: along the normal to the (100) surface in the case of Si(100) and at an angle to the sur-

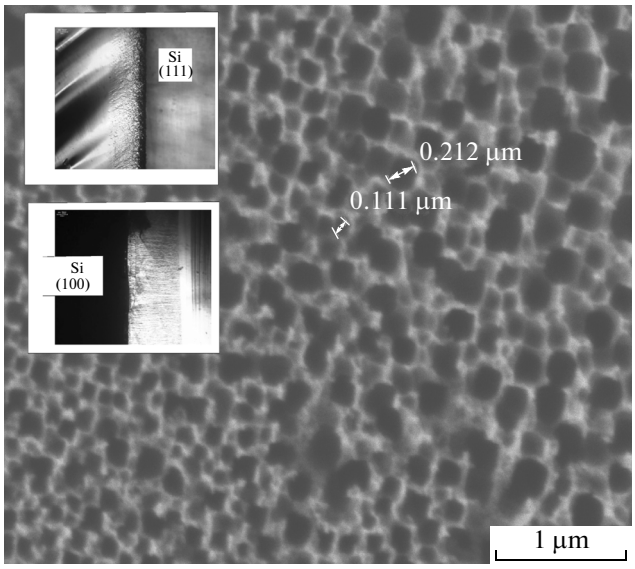

Fig. 11. SEM image of the surface of an NS layer produced on KEF 0.7 and photographs of fracture surfaces: etching current, 25 mA/cm^2; etching time, 30 min.

face in the case of Si(111), which underlies the tendency of the pores to have a square shape (Figs. 4, 5, 11).

CONCLUSIONS

The donor impurity content influences the structuring of NS layers and the pore distribution density in *n*-Si.

The participation of the $(HF_2)^-$ ion in electrochemical etching possibly accounts for the pore shape and the influence of the crystallographic orientation of the substrate on the spatial orientation of the pores.

The low probability of simultaneous interaction of the two fluorine atoms of a $(HF_2)^-$ ion with silicon atoms seems to account for the discrepancy between the experimentally determined and calculated radial nanopore sizes.

Nanoporous silicon layers produced on *p*- and *n*-type silicon substrates under identical conditions differ in mechanical strength, thickness, and stability to external influences, which is probably related to distinctions between their structures.

Varying the preparation conditions of NS layers makes it possible to obtain NS with tailored parameters (axial and radial pore sizes and pore distribution density), which offers the possibility of using it in devices for various practical applications.

ACKNOWLEDGMENTS

This work was supported by the RF Ministry of Education and Science, state research target no. 2014/114, project no. 150.

REFERENCES

1. Ksenofontova, O.I., Vasin, A.V., Egorov, V.V., Bobyl', A.V., Soldatenkov, F.Yu., Terukov, E.I., Ulin, V.P., and Kiselev, O.I., Porous silicon and its applications in biology and medicine, *Tech. Phys.*, 2014, vol. 84, no. 1, pp. 66–77.
2. Belous, A.O., Biomedical applications of porous silicon, *Molodoi Uchenyi*, 2013, no. 8, pp. 69–74.
3. Ishchenko, A.A., Fetisov, G.V., and Aslanov, P.A., *Nanokremnii: svoistva, poluchenie, primenenie, metody ispol'zovaniya i kontrolya* (Nanosilicon: Properties, Preparation, Applications, and Techniques for Use and Control), Moscow: FIZMATLIT, 2011.
4. Gavrilov, S.A. and Belov, A.N., *Elektrokhimicheskie protsessy v tekhnologii mikro- i nanoelektroniki* (Electrochemical Processes in Micro- and Nanoelectronics Technologies), Moscow: RIOR INFRA-M, 2014.
5. Yuzova, V.A., Levitskii, A.A., and Kharlashin, P.A., Advances in the preparation and characterization of porous silicon, *J. Sib. Fed. Univ. Eng. Technol.*, 2011, vol. 4, pp. 92–112.
6. Churaman, W.A. and Currano, L., Preparation of nanoporous silicon, *Army Res. Lab.*, 2012, p. 22.
7. Goryachev, D.N., Belyakov, L.V., and Sreselli, O.M., Electrolytic fabrication of porous silicon with the use of internal current source, *Semiconductors*, 2003, vol. 37, no. 4, pp. 477–481.
8. Tynyshtykbaev, K.B., Ryabikin, Yu.A., Tokmoldin, S.Zh., Aitmukan, T., Rakymetov, B.A., and Vermenichev, R.B., Morphology of porous silicon after long-term internal current source anodic etching in electrolyte, *Fiz. Tekh. Poluprovodn.* (S.-Peterburg), 2010, vol. 36, no. 11, pp. 104–110.
9. Zalkind, Ya.G., Physicomathematical properties of silicon nanostructures as a technologically attractive material for microcircuit engineering, *Cand. Sci. (Chem.) Dissertation*, Moscow, 2006.
10. Abramova, E.N., Gvelesiani, A.A., Khort, A.M., and Yakovenko, A.G., Effect of the content of hydrogen fluoride in an etchant on the formation of nanopores in silicon during electrolytic etching, *Russ. J. Inorg. Chem.*, 2014, vol. 59, no. 11, pp. 1328–1332.
11. Kompan, M.E., Mechanism of primary self-organization of the regular structure of porous silicon, *Fiz. Tekh. Poluprovodn.* (S.-Peterburg), 2003, vol. 45, no. 5, pp. 1130–1134.
12. Akhmetov, N.S., *Neorganicheskaya khimiya* (Inorganic Chemistry), Moscow: Vysshaya Shkola, 1988.
13. Rabinovich, V.A. and Khavin, Z.Ya., *Kratkii spravochnik khimika* (Concise Chemist's Handbook), Leningrad: Khimiya, 1977.
14. Seeger, K., *Semiconductor Physics*, New York: Springer, 1977.

Translated by O. Tsarev